A determination of the structure of liquid Ag_2Se using neutron diffraction and isotopic substitution

1997 J. Phys.: Condens. Matter 9 6159

(http://iopscience.iop.org/0953-8984/9/29/002)

J. Phys.: Condens. Matter **9** (1997) 6159–6173. Printed in the UK PII: S0953-8984(97)84181-1

A determination of the structure of liquid Ag_2Se using neutron diffraction and isotopic substitution

A C Barnes†, S B Lague†, P S Salmon‡ and H E Fischer§

† H H Wills Physics Laboratory, University of Bristol, Bristol BS8 1TL, UK
‡ School of Physics, University of East Anglia, Norwich NR4 7TJ, UK
§ Institut Laue–Langevin, Avenue des Martyrs, F-38042, Grenoble, France

Received 14 May 1997

Abstract. The partial structure factors and pair distribution functions for liquid Ag_2Se were measured using the method of neutron scattering and isotopic substitution. The results show many features which are consistent with an ionic melt in which small Ag^+ ions move rapidly through a highly ordered Se^{2-} liquid sub-structure in a similar way to the motion of Ag^+ in the fast-ion solid which exists prior to melting. The results are compared with recent molecular dynamics and *ab initio* molecular dynamics calculations, and the relative merits of the two simulation approaches are discussed in relation to the data.

1. Introduction

The silver chalcogenide compounds Ag_2X (X = S, Se or Te) are materials of considerable fundamental and technological interest in both their solid and liquid states. In their solid phases they not only become fast-ion conductors at moderate temperatures (due to motion of Ag^+ through the lattice; Kobayashi 1990), but also show a significant electronic contribution to their total electrical conductivity (Hasegawa 1985). For many years, understanding their electronic properties in both the crystalline and liquid states has proved to be particularly difficult. For example, as the composition of molten Ag–S or Ag–Se alloys is changed an anomalous increase in the electrical conductivity σ is observed precisely at the stoichiometric composition Ag_2X (Endo *et al* 1980, Ohno *et al* 1990, 1994). The stoichiometric composition is also notable as having a negative temperature coefficient of the conductivity, $d\sigma/dT$, in marked contrast to other liquid semiconductors with comparable conductivities. In contrast, this behaviour is not seen for liquid Ag–Te whose properties are much closer to those of typical liquid semiconductors (Enderby and Barnes 1990). Recently, a new impetus for understanding such systems has come from studies of the liquid and solid phases of these and other materials which show both rapid ionic motion and a significant electronic conductivity in their solid phases (Kobayashi 1990). The general conclusions suggest that the effects of the ionic motion must be included in any discussion of the electronic properties of this class of material. It was pointed out by Huberman (1974) and Ramasesha (1982) that it is possible to show, using thermodynamic arguments, how the ionic motion could couple to the electronic density of states and hence affect the electronic conductivity.

The relationship between the ionic mobility of Ag^+ and the electronic conductivity is also important when considering the properties of silver chalcogenide glasses. When

0953-8984/97/296159+15$19.50

Ag_2X is mixed with a network former such as AsX or As_2X_3 to form, for example, glassy $(Ag_2Se)_{0.25}(AsSe)_{0.75}$ or $(Ag_2Te)_{0.5}(As_2Te_3)_{0.5}$ the resultant material is sometimes a fast-ion conductor and sometimes a semiconductor. It is found, however, that irrespective of the mechanism for the electrical conductivity in the glass, the short-range order of the network former is not destroyed and that elements of the short- and intermediate-range order of the network modifier Ag_2X are retained (Benmore and Salmon 1994, Salmon and Liu 1996). These results lend support to a modified random-network-type model for the structure (Greaves *et al* 1991) in which the network formers and modifiers preserve some features of their characteristic ordering to form two interlacing networks. It is therefore important to have information on the Ag_2X structure at the partial pair distribution function level if realistic models of the glass structure and its interrelation with the electrical conductivity are to be developed.

In this paper we present an accurate measurement for the partial structure factors of liquid Ag_2Se using the method of neutron diffraction and isotopic substitution. The results are first discussed in terms of their relation with other molten systems for which partial structure factors are available. This is of significance because the results for Ag_2Se are some of the first for a melt in which the cation-to-anion ratio is 2:1. Next, the local coordination environments of the atomic species are compared with those in the high-temperature superionic crystalline phases from which the Ag_2X compounds melt. The merits of recent molecular dynamics (MD) and *ab initio* molecular dynamics (AIMD) simulations on the Ag_2Se system are then compared. Finally the interrelation between the melt structure and its electrical properties are discussed.

Table 1. Neutron scattering parameters used in the data analysis.

Isotope	$\bar{b}$ (fm)	σ_a (at 0.7 Å) (b)	σ_s (b)
^{N}Ag	5.922 ± 0.007	24.6 ± 0.2	4.99 ± 0.03
^{107}Ag	7.64 ± 0.04	14.6 ± 0.5	7.44 ± 0.09
^{109}Ag	4.19 ± 0.03	35.4 ± 0.4	2.55 ± 0.06
^{N}Se	7.97 ± 0.02	4.55 ± 0.08	8.31 ± 0.06
^{76}Se	12.2 ± 0.1	33.1 ± 2.7	18.7 ± 0.3

2. Experimental procedure

An experiment to measure the partial structure factors of liquid Ag_2Se at 1273 K was carried out using the D4B liquids diffractometer at the High Flux Beams Reactor at the Institut Laue–Langevin, Grenoble, France. Three isotopically labelled samples of Ag_2Se ($^{107}Ag_2{}^{76}Se$, $^{109}Ag_2{}^{N}Se$ and $^{N}Ag_2{}^{76}Se$ where N indicates the natural isotopic abundance) were prepared by mixing the pure elements in a quartz ampoule and then heating them to 1350 K in a rocking furnace to ensure a complete reaction. The samples were then transferred to matched thin-walled silica tubes with an internal diameter of $\sim$4 mm and a wall thickness of 0.4 mm prior to being sealed under vacuum for use in the diffraction experiments. The standard D4B furnace with a tubular vanadium heater of thickness 0.1 mm was used for all of the measurements. Diffraction patterns were measured for the background (nothing at the sample position), a cadmium bar having the same dimensions as the sample, the empty furnace, a vanadium calibration bar, the empty silica tube (at 1273 K) and the three samples. Each diffraction pattern was built up by making repeated scans of the detectors over the available range of scattering angles. No deviation was observed between scans, apart

from the expected statistical variations, which verified the stability of both the samples and the instrument (Jal *et al* 1990). Corrections were applied for the background (Bertagnolli *et al* 1976), self-attenuation (Paalman and Pings 1962, Poncet 1977, 1978), multiple scattering (Blech and Averbach 1965, Soper and Egelstaff 1980) and inelasticity effects (Yarnell *et al* 1973). The incident neutron wavelength used was 0.7 Å and the values of the bound coherent scattering lengths, $\bar{b}$, absorption cross-sections, σ_a, and scattering cross-sections, σ_s, used in the data analysis are given in table 1. The neutron scattering lengths and cross-sections for silver and selenium were taken from Koester and Knopf (1980) and Koester *et al* (1980) respectively. The bulk number density of the sample was taken to be 0.044 Å^{-1} as determined by Tsuchiya (1996) and Czack *et al* (1983). This density was consistent, within error, with the neutron scattering lengths and cross-sections used in the data analysis.

The total structure factors $F(Q)$ which resulted from the initial correction procedures did not oscillate about the correct high-Q limit, where Q is the scattering vector, and did not give rise to real-space functions which oscillated around their correct low-r limit. The source of this problem was traced to a tendency of the molten samples to form small bubbles such that the total number of scattering centres was less than expected and could not be calculated accurately. The $F(Q)$ functions were therefore scaled to be consistent with their correct high-Q limits. The scaling factors necessary were in accordance with the density of bubbles in the liquid samples as estimated from the number of small voids in the solidified samples.

The $F(Q)$s for the different isotopic compositions can be decomposed into weightings of the Faber–Ziman partial structure factors, $S_{ij}(Q)$, and written in matrix form as

$$\begin{pmatrix} {}^{107}_{\text{N}}F(Q) \\ {}^{109}_{76}F(Q) \\ {}^{\text{N}}_{76}F(Q) \end{pmatrix} = \begin{pmatrix} 0.2594 \pm 0.0019 & 0.0706 \pm 0.0001 & 0.2706 \pm 0.0014 \\ 0.0780 \pm 0.0008 & 0.1654 \pm 0.0019 & 0.2272 \pm 0.0025 \\ 0.1559 \pm 0.0003 & 0.1654 \pm 0.0019 & 0.3211 \pm 0.0027 \end{pmatrix} \times \begin{pmatrix} S_{\text{AgAg}}(Q) - 1 \\ S_{\text{SeSe}}(Q) - 1 \\ S_{\text{AgSe}}(Q) - 1 \end{pmatrix} \tag{1}$$

where the $F(Q)$s are expressed in barns (1 b $= 10^{-28}$ m^2). The $S_{ij}(Q)$ can be obtained from inversion of this matrix to give

$$\begin{pmatrix} S_{\text{AgAg}}(Q) - 1 \\ S_{\text{SeSe}}(Q) - 1 \\ S_{\text{AgSe}}(Q) - 1 \end{pmatrix} = \begin{pmatrix} 12.17 & 17.31 & -22.50 \\ 8.11 & 32.22 & -29.63 \\ -10.09 & -25.00 & 29.30 \end{pmatrix} \begin{pmatrix} {}^{107}_{\text{N}}F(Q) \\ {}^{109}_{76}F(Q) \\ {}^{\text{N}}_{76}F(Q) \end{pmatrix}. \tag{2}$$

A measure of the conditioning of this matrix is given by its normalized determinant $|A_n| = 0.029$ (Edwards *et al* 1975). The partial pair distribution functions, $g_{ij}(r)$, were obtained from the corresponding $S_{ij}(Q)$ by Fourier transformation. It was found that the first set of scaled $F(Q)$s gave rise to $g_{ij}(r)$ showing a small peak at 1.6 Å which corresponds to the Si–O bond length and represents a small contamination from the silica containers (no bond distances of less than 2 Å are expected for Ag_2Se). By measuring the height of this peak in each of the $g_{ij}(r)$ it was possible, by re-inverting the scattering matrix, to calculate the additional silica cell subtraction required on each of the $F(Q)$s to completely remove the container scattering from the data. This additional correction was very small and amounted to less than one per cent of the original container scattering. The resulting functions were renormalized and the fully corrected $F(Q)$s, which are illustrated in figure 1, were used in equation (2) for extracting the partial structure factors.

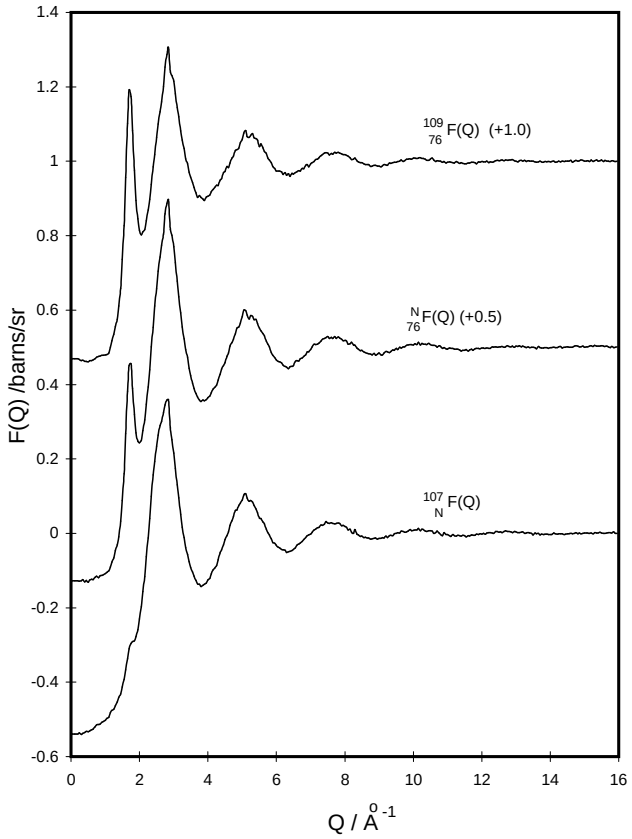

Figure 1. The fully corrected experimental total structure factors for liquid Ag_2Se.

Table 2. Interatomic distances and coordination numbers in liquid Ag_2Se.

$g_{ij}(r)$	First-peak distance (Å)	Second-peak distance (Å)	$\bar{n}_i^j$
$g_{SeSe}(r)$	4.6 ± 0.1	8.1 ± 0.3	13.0 ± 0.5
$g_{AgSe}(r)$	2.60 ± 0.05	6.2 ± 0.5	9.3 ± 0.5
$g_{AgAg}(r)$	2.80 ± 0.05	5.0 ± 0.5	5.3 ± 0.5

3. Results

Figure 2 shows, as error bars, the $S_{ij}(Q)$, obtained by direct inversion, using equation (2), of the fully corrected $F(Q)$s shown in figure 1 and, as smooth lines, the cubic spline fits to these $S_{ij}(Q)$. The corresponding $g_{ij}(r)$ are shown in figure 3 as dashed and full lines respectively. The measured partial structure factors fully satisfy the sum rules and inequality relations given by Edwards *et al* (1975) and give $g_{ij}(r)$ which oscillate around the correct low-r limit. A summary of the mean atomic distances and coordination numbers obtained from the $g_{ij}(r)$ is given in table 2, where $\bar{n}_i^j$ denotes the mean number of species j around species i as evaluated by integrating over $g_{ij}(r)$ to its first minimum. Figure 4 shows the $F(Q)$s decomposed as the Bhatia–Thornton partial structure factors, $S_{ij}^{BT}(Q)$ (Bhatia

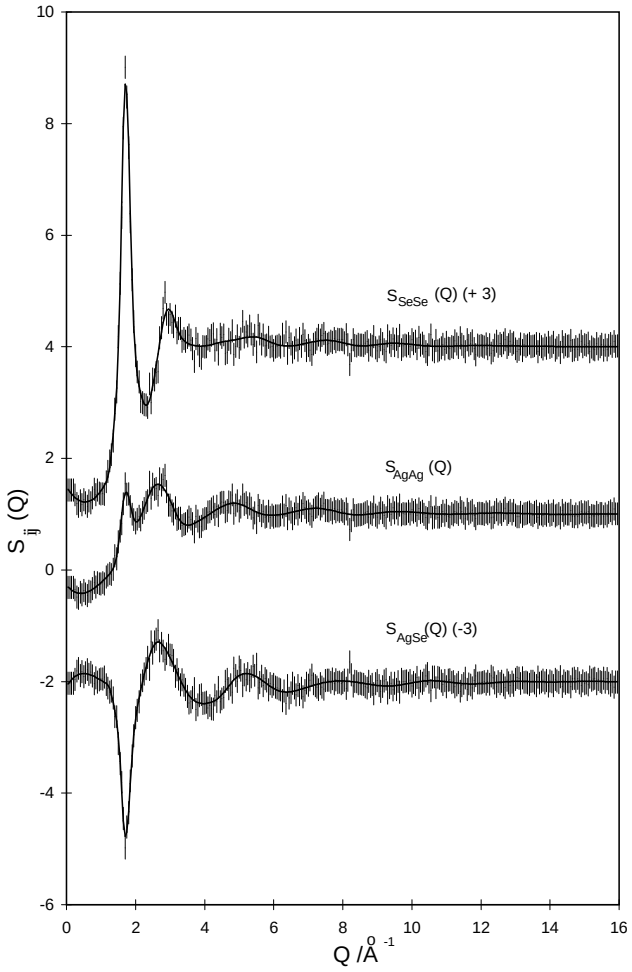

Figure 2. The experimental partial structure factors $S_{\mathrm{SeSe}}(Q)$, $S_{\mathrm{AgAg}}(Q)$ and $S_{\mathrm{AgSe}}(Q)$. The error bars indicate the statistical errors on the data points. The solid lines are the smoothed $S_{ij}(Q)$ obtained by using a cubic spline fit to the data points.

and Thornton 1970). $S_{NN}^{BT}(Q)$, $S_{NC}^{BT}(Q)$ and $S_{CC}^{BT}(Q)$ are the number–number, number–concentration and concentration–concentration partial structure factors respectively. The Fourier transform of $S_{NN}^{BT}(Q)$, $g_{NN}(r)$, describes the sites of the scattering nuclei and does not distinguish between the different chemical species. It is therefore measured directly if the bound coherent scattering lengths of the nuclei are equal. This is almost the case for the $^{107}Ag_2{}^{\mathrm{N}}Se$ measurement (table 1), and hence $S_{NN}^{BT}(Q)$ is known to good precision.

4. Discussion

4.1. Comparison with the structure of molten salts

The partial structure factors for several binary systems have been measured for which the ratio of the number of electropositive to that of electronegative species is 1:1 or 1:2 (see e.g. Rovere and Tosi 1986, Salmon 1992). It is therefore of interest to compare the structure

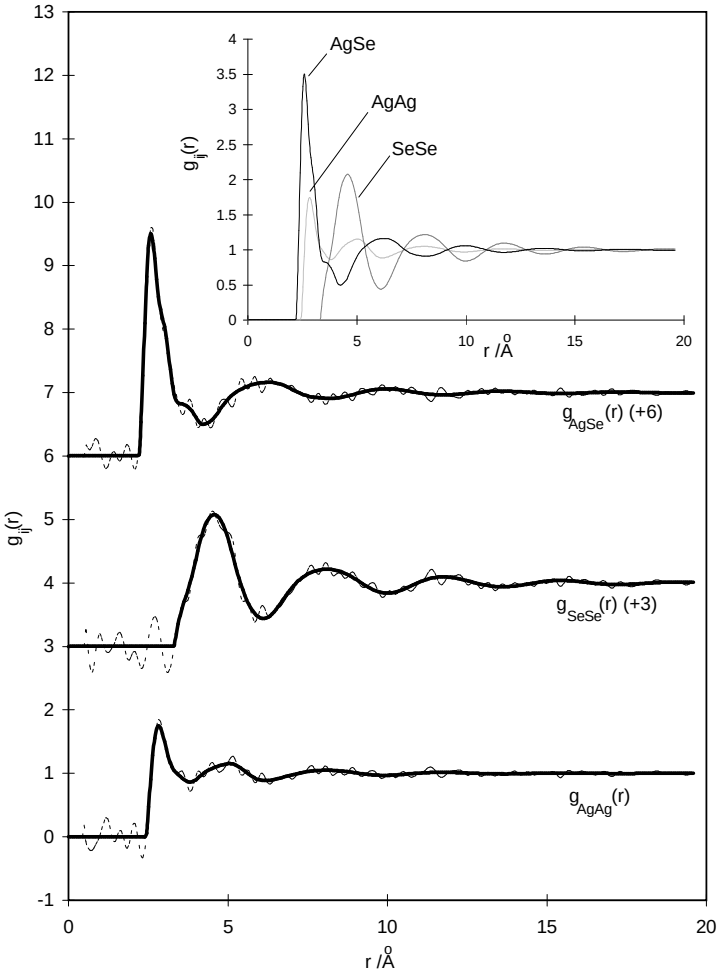

Figure 3. The $g_{ij}(r)$ obtained from the $S_{ij}(Q)$ shown in figure 2. The solid lines are the Fourier transforms of the smoothed $S_{ij}(Q)$, and the broken lines are the Fourier transforms of the unsmoothed $S_{ij}(Q)$. The inset shows the smoothed $g_{ij}(r)$ superimposed on the same axis.

of these systems with that of molten Ag_2Se for which the corresponding ratio is 2:1. The only other reported measurements for a 2:1 system, molten Cu_2Te (Hawker *et al* 1974), are old and are of insufficient quality to effect a reliable comparison.

The $S_{ij}(Q)$ for Ag_2Se show several features which are consistent with a large electronegativity difference between the chemical species (Rovere and Tosi 1986). Firstly, there is a pronounced dip at $\sim$1.8 Å^{-1} in $S_{\mathrm{AgSe}}(Q)$ which occurs at the same position as a strong peak in $S_{\mathrm{SeSe}}(Q)$ and a much weaker peak in $S_{\mathrm{AgAg}}(Q)$. These features combine to give a prominent peak in $S_{CC}^{BT}(Q)$ at 1.8 Å^{-1} which is higher ($\sim$0.75) than the corresponding feature observed for both $SrCl_2$ (0.6) and $BaCl_2$ (0.5) (Salmon 1992) and implies pronounced chemical ordering. This ordering can also be observed in the long-ranged concentration fluctuations shown in $g_{CC}(r)$, the real-space representation of $S_{CC}^{BT}(Q)$ (see the inset to figure 4). Secondly, the low-Q limit of zero indicated by the measured $S_{CC}^{BT}(Q)$ is consistent with the electroneutrality and complete screening conditions which

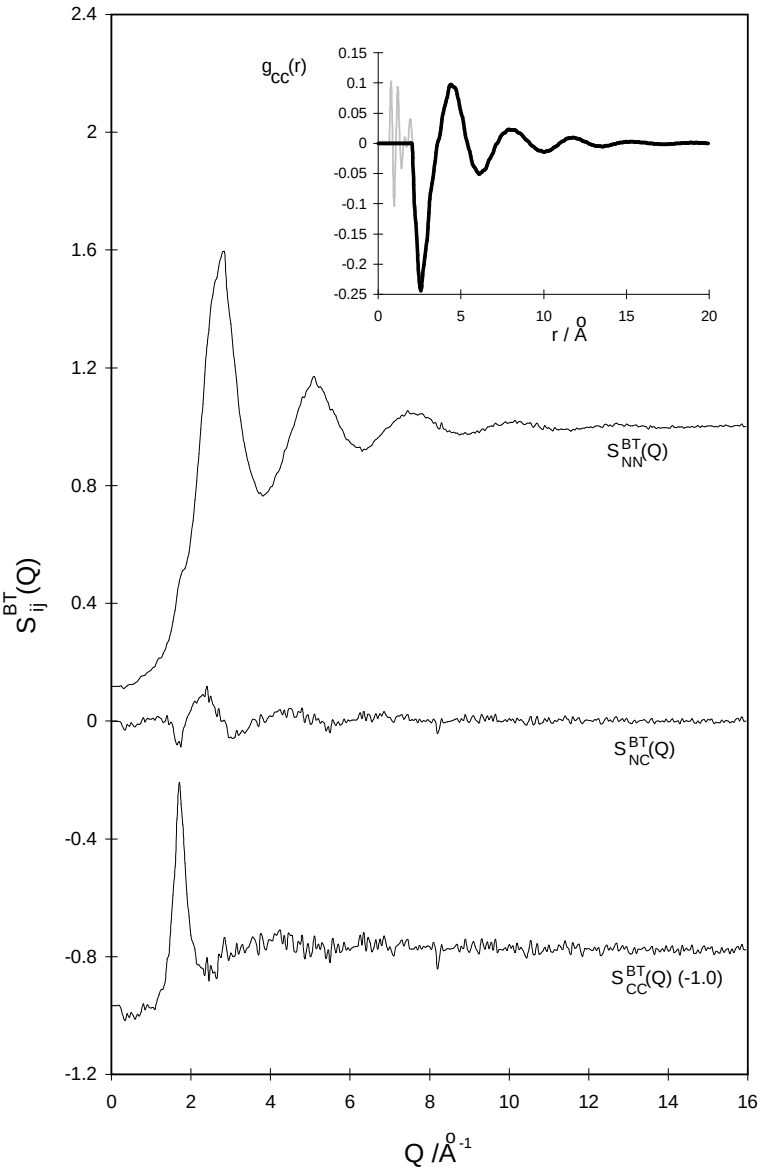

Figure 4. The experimental Bhatia–Thornton partial structure factors $S_{ij}^{BT}(Q)$. The inset shows the real-space Fourier transform $g_{CC}(r)$ of $S_{CC}^{BT}(Q)$.

apply to an ionic liquid (Stillinger and Lovett 1968, Bhatia 1977, Rovere and Tosi 1986). Thirdly, $S_{CC}^{BT}(Q)$ for Ag_2Se does not have a first sharp diffraction peak at ~ 1 Å^{-1} unlike the case of the glass-forming network melts such as $ZnCl_2$ (Biggin and Enderby 1981) and $GeSe_2$ (Penfold and Salmon 1991). However, there is a close similarity to the measured $S_{CC}^{BT}(Q)$ for molten $SrCl_2$ and $BaCl_2$ for which the bond ionicity is much higher (Rovere and Tosi 1986).

In real space, there is a strong overlap between $g_{\mathrm{AgSe}}(r)$ and $g_{\mathrm{AgAg}}(r)$ at low r, i.e. the first coordination shell for heteropolar contacts is penetrated by the first coordination shell

for the like atom species which are mobile in the superionic phase. A similar observation is made for $SrCl_2$ and $BaCl_2$ which both melt from superionic phases in which chlorine is the mobile species, i.e. the first coordination shells for Sr–Cl and Ba–Cl overlap with that for Cl–Cl (Edwards *et al* 1978, McGreevy and Mitchell 1982). Strong overlap between the first coordination shells defined by the heteropolar and homopolar $g_{ij}(r)$ is *not*, however, observed for 1:2 melts such as $ZnCl_2$ and $GeSe_2$ in which the bond ionicity is smaller. The measured $g_{ij}(r)$ for Ag_2Se also show the characteristic features of charge ordering for ionic melts in the respect that $g_{AgAg}(r)$ and $g_{SeSe}(r)$ are in antiphase to $g_{AgSe}(r)$ for $r \gtrsim 7$ Å. Charge cancellation also occurs, i.e., if we assign formal charges of $+1$ and -2 to Ag and Se respectively, the net charge around any one species cancels when $r \gtrsim 7$ Å. Overall, the structure of molten Ag_2Se has many features which are reminiscent of binary ionic liquids.

4.2. Comparison with the Ag_2X crystal structure prior to melting

Enderby and Barnes (1990) have discussed how the structure of a solid just before melting can prove a useful guide to the local coordination in the melt. In the case of Ag_2Se, the solid melts at 1170 K from a fast-ion phase in which the silver atoms are the mobile species within a body-centred cubic (b.c.c.) lattice of selenium atoms (Kobayashi 1990). For the closely related compound Ag_2S, there is a change in structure at 866 K from a fast-ion phase, in which silver moves through a sulphur b.c.c. lattice, to another fast-ion phase, in which silver moves through a sulphur face-centred cubic (f.c.c.) lattice before melting at 1115 K. This suggests that the local structures of both the b.c.c. and f.c.c. solids may be considered as possible starting points for discussing liquid Ag_2Se. In the following discussion we will consider the positions and coordination numbers for these two lattice types and compare them with the observed peak positions and coordination numbers for the liquid. In so doing, we will use crystal lattice parameters that give the same number density as the liquid. This criterion gives lattice parameters of 5.14 Å and 6.49 Å for the b.c.c. and f.c.c. structures respectively. It should be noted that even a 10% change in this number density only results in a 3% change in the predicted distances.

In the b.c.c. structure each Se atom is surrounded by 8 Se at 4.45 Å, 6 Se at 5.14 Å, 12 Se at 7.27 Å, 24 Se at 8.52 Å and 8 Se at 8.90 Å. The most favourable positions for the Ag^+ ions are four out of the twelve tetrahedral vacancies in the selenium lattice which give rise to Ag–Se distances of 2.87 Å and 4.63 Å. However, the Ag^+ ions are free to move between these tetrahedral sites via the six octahedral or twenty four triangular sites of the b.c.c. lattice (see figure 5). These give Ag–Se distances of $\sim$2.6 Å and 3.6 Å (octahedral sites) and $\sim$2.7 Å (triangular sites).

In the f.c.c. structure each Se atom is surrounded by 12 Se at 4.59 Å, 6 Se at 6.49 Å, 24 Se at 7.95 Å and 12 Se at 9.18 Å. The most favourable positions for the Ag^+ ions are the eight tetrahedral sites of the anti-fluorite structure which give rise to a Ag–Se nearest-neighbour distance of 2.81 Å. These sites would be fully occupied for Ag_2Se. However, there are also 4 empty octahedral sites in the unit cell that can also accommodate the silver ions and which allow the fast-ion motion. These give a nearest-neighbour Ag–Se distance of 3.25 Å. The Ag^+ ions move between these sites via 32 triangularly coordinated sites which give a minimum Ag–Se distance of $\sim$2.7 Å.

In the liquid state, the positions of the first two peaks in $g_{SeSe}(r)$ are at $\sim$4.5 Å and $\sim$8.0 Å which are consistent with either a local b.c.c. or f.c.c. arrangement of Se atoms given the breadth of the peaks. The nearest-neighbour coordination number of 13.0 ± 0.5 determined by calculating to the first minimum in $g_{SeSe}(r)$ is lower than the composite coordination number of 14 expected from the first- and second-nearest-neighbour distances

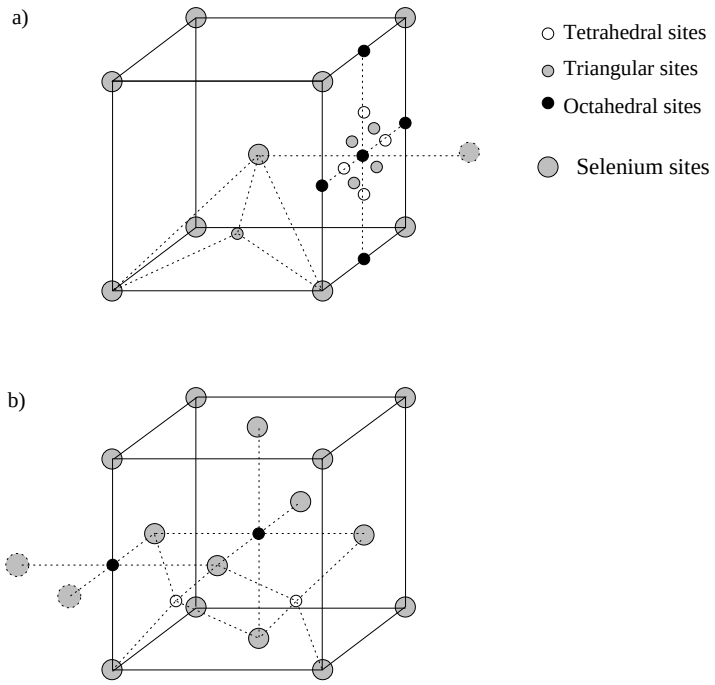

Figure 5. Diagrams to show representative examples of the positions of (a) the triangular, tetrahedral and octahedral sites in the body-centred cubic lattice, and (b) the octahedral and tetrahedral sites in the face-centred cubic structure. The Se atoms are denoted as the large shaded circles.

in the b.c.c. structure (4.26 Å and 5.27 Å), and higher than the value of 12 expected for the f.c.c. structure. Other methods for determining the nearest-neighbour coordination number (namely reflection of the first peak about its maximum and fitting gaussians up to the first minimum in $g_{\mathrm{SeSe}}(r)$) also give values less than 14. As there is a general tendency to lower coordination numbers in the liquid state (see e.g. McGreevy and Pusztai 1990) this suggests that the local structure in molten Ag_2Se is most closely related to that of the b.c.c. structure from which it melts.

The first peak in $g_{\mathrm{AgSe}}(r)$ occurs at ∼2.6 Å which is smaller than the value of 2.8 Å that is predicted for the tetrahedral sites in both the b.c.c. and f.c.c. structures. It is, however, comparable to the distances expected for occupation of the octahedral and triangular sites of the b.c.c. lattice and the triangular sites of the f.c.c. lattice, but not of the octahedral sites of the latter.

$g_{\mathrm{AgAg}}(r)$ shows a well defined distance of 2.8 Å which corresponds to the separation between several of the tetrahedral and octahedral sites in both the f.c.c. and b.c.c. structures, and a second peak at ∼4.5–5.0 Å. There is weak minimum between these peaks which is consistent with a rapid movement of the silver ions in the liquid and/or a large distribution of sites of different symmetries.

4.3. Comparison with computer simulations

It is interesting to compare the partial structure factors obtained in this work with those of recent computer simulations. Rino *et al* (1988) have carried out extensive molecular

dynamics (MD) simulations on the Ag_2Se system, including the solid fast-ion and molten phases, using semi-empirical ionic potentials which contain three adjustable terms, namely:

(i) a Coulomb interaction $Q_i Q_j / r_{ij}$, where Q_i is the effective charge on the ith ion;
(ii) a charge dipole interaction which includes the electronic polarizability of the ith ion and a screening term;
(iii) a steric repulsion term to balance the attractive Coulomb interaction between cations and anions at short distances.

In the simulations, the polarizability of the cation was neglected to eliminate term (ii) in the Ag–Ag interaction, and the effective ionic charges were chosen to be considerably smaller that the formal charges of $+1$ and -2 for Ag and Se respectively.

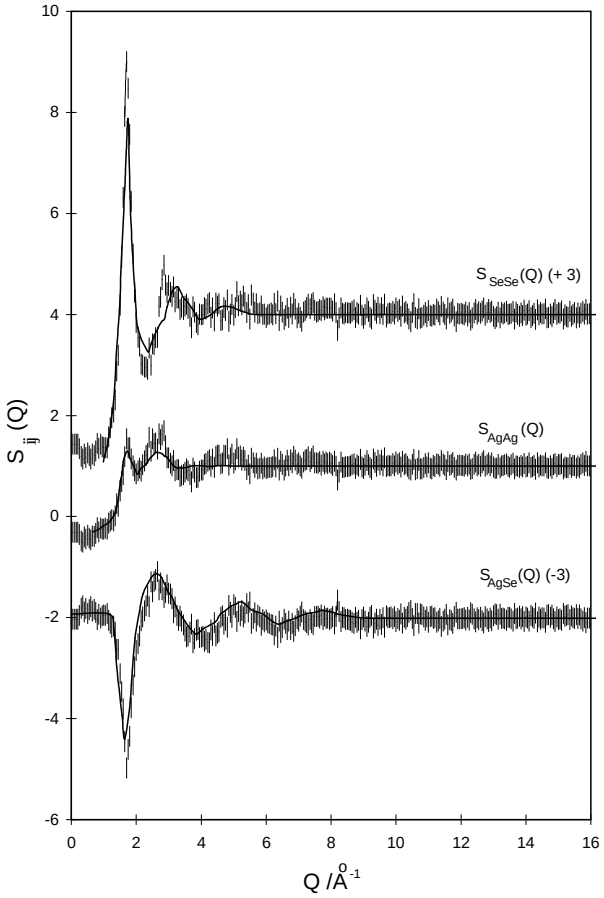

Figure 6. The experimental $S_{ij}(Q)$ (error bars) compared with the $S_{ij}^{MD}(Q)$ (solid lines) obtained in the molecular dynamics simulation of Rino *et al* (1988).

Figure 6 shows the experimental partial structure factors and those obtained in the MD simulations of Rino *et al* (1988). The corresponding real-space functions are shown in figure 7. The level of agreement with experiment is good, particularly for $S_{\mathrm{AgSe}}^{MD}(Q)$ and $S_{\mathrm{SeSe}}^{MD}(Q)$. However, there is more structure in the experimental $S_{\mathrm{AgAg}}(Q)$ at high Q than is found for $S_{\mathrm{AgAg}}^{MD}(Q)$, which indicates that the short-range Ag–Ag correlations are much

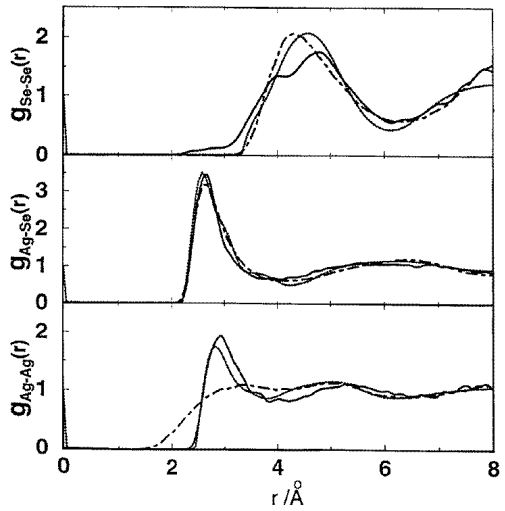

Figure 7. A comparison of the experimental $g_{ij}(r)$ for liquid Ag_2Se (dotted lines) with those of the *ab initio* molecular dynamics simulation of Kirchhoff *et al* (1996) (solid lines) and the molecular dynamics simulations of Rino *et al* (1988) (chain lines).

stronger than given by the simulation. In real space this is seen in $g_{\mathrm{AgAg}}(r)$ as a peak at 2.8 Å which is notably higher and sharper than that seen in $g^{MD}_{\mathrm{AgAg}}(r)$ (see figure 7). This suggests that the polarizability of silver should not have been neglected in the MD simulations. Further, the conductivity of Ag_2Se just after melting approaches 500 Ω^{-1} cm^{-1}, some two orders of magnitude higher than the typical ionic conductivity of a molten salt, and only one order of magnitude less than those of some liquid metals (Ohno *et al* 1994). This is indicative of a substantial number of itinerant electrons in the system, and the choice of parameters in the effective potentials presumably has the effect of accounting for the screening effect of these electrons in a mean-field manner.

More recently a full *ab initio* molecular dynamics (AIMD) simulation for liquid Ag–Se at several compositions has been carried out by Kirchhoff *et al* (1996). The AIMD technique has the advantage that the forces on the ions are calculated using first-principles quantum methods with no adjustable parameters, except for the establishment of suitable atom core pseudopotentials. At the same time the atomic dynamics and the electronic structure are calculated in a self-consistent way. It is the ability to calculate the electronic density of states which is particularly important in understanding liquid semiconducting systems in which mixed conduction takes place. It is also possible, and important for understanding the electronic properties of binary systems, to treat off-stoichiometric compositions using the same method. Despite these advantages there are several important limitations of the AIMD method as applied to liquid Ag_2Se:

(i) the number of atoms in the simulation was restricted to 69;

(ii) assumptions had to be made to account for the rather localized 4d band in terms of the finite plane-wave basis set;

(iii) assumptions were made regarding the atomic configuration;

(iv) the local density approximation is poor for calculations of band-gap properties.

Further, the simulation times were very small compared with those in conventional MD methods.

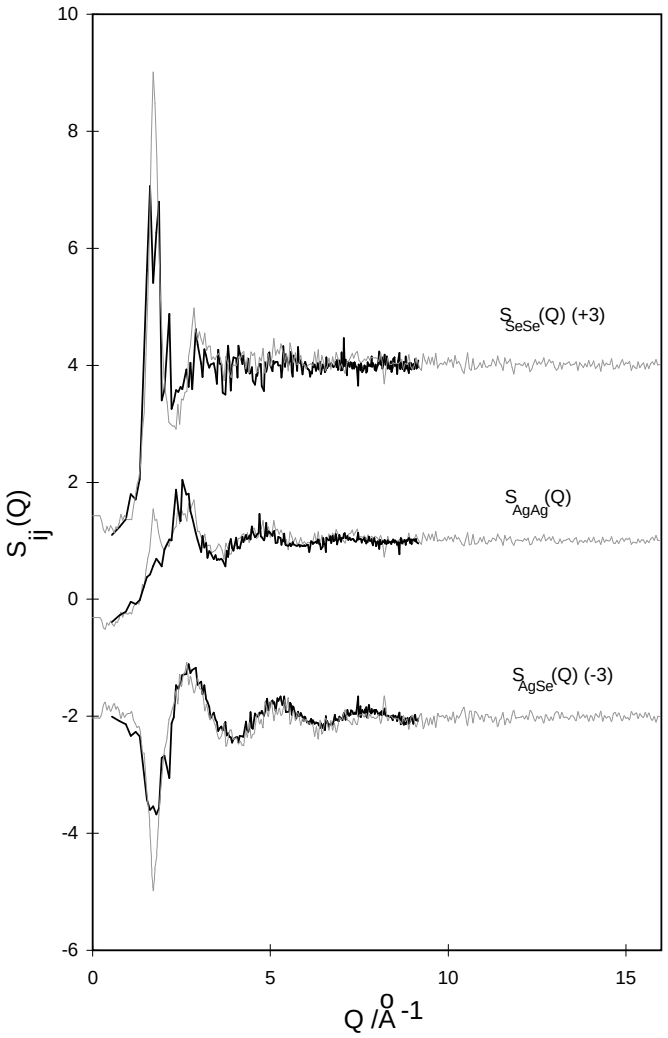

Figure 8. The experimental $S_{ij}(Q)$ (broken lines) compared with the $S_{ij}^{AIMD}(Q)$ (solid lines) obtained in the *ab initio* molecular dynamics simulation of Kirchhoff *et al* (1996).

Figure 8 compares the experimental partial structure factors with those obtained in the AIMD simulations of Kirchhoff *et al* (1996). The corresponding real-space functions are shown in figure 7. For $Q \gtrsim 2$ Å^{-1}, there is good agreement between the experimental data and the simulation results (the noise on the $S_{ij}^{AIMD}(Q)$ is due to the small number of atoms in the simulations and the small number of time steps that can currently be achieved). Most noticeable is the much better agreement with experiment in the high-Q region for $S_{\mathrm{AgAg}}^{AIMD}(Q)$ than for $S_{\mathrm{AgAg}}^{MD}(Q)$ which suggests that the AIMD method is better able to deal with the itinerant electrons at short distances. However, for $Q \lesssim 2$ Å^{-1} there are clear discrepancies between experiment and the AIMD results for all three partial structure factors. For example:

(i) the first peak in $S_{\mathrm{SeSe}}^{AIMD}(Q)$ is less intense and broader than observed in both the experiment and MD simulation;

(ii) the 'charge-ordering dip' at $\simeq 1.8$ Å^{-1} in $S_{\mathrm{AgSe}}^{AIMD}(Q)$ is smaller than it is in the

experiment;

(iii) there is a complete absence in $S^{AIMD}_{AgAg}(Q)$ of the experimental peak observed at $\simeq 1.8$ Å^{-1}.

There are, therefore, inadequacies of the present AIMD simulations which are most prevalent at large distances. Nevertheless, the calculated electronic structure shows a deep pseudo-gap in the electronic density of states and gives an electronic conductivity which is similar to the experimental value.

4.4. The relation between the structure and electronic properties of the melt

The experimental data and the simulation results confirm the basic picture of liquid Ag_2Se as a quasi-ionic liquid semiconductor with an essentially zero conductivity gap ΔE (Enderby and Barnes 1990). For this type of liquid semiconductor the electrical conductivity is predicted to be a minimum at stoichiometry and to show a positive temperature coefficient $d\sigma/dT$ (Barnes 1993). However, experimentally Ag_2Se shows exactly the opposite behaviour (Ohno *et al* 1994). It is also surprising that liquid Ag_2Te, which shows more conventional liquid semiconducting behaviour, is structurally (at least to the total structure factor level) very similar to Ag_2Se (Price *et al* 1993). From measurements of the electronic properties (electrical conductivity, thermopower and magnetic susceptibility) of Ag_2Se (Ohno *et al* 1994) it was concluded that the enhanced conductivity at stoichiometry was due to an enhanced carrier mobility rather than an increase of the carrier density. Recently it has been suggested (Fortner *et al* 1995) that the unusual carrier enhancement observed in solid NaSn and CsPb could be due to a coupling between highly mobile ions and electrons in a manner outlined by Ramasesha (1982). We believe that a similar mechanism may be the origin of the unusual electronic properties of liquid Ag_2Se. Support for this argument has also been found in the recent discovery that Mg_3Bi_2, another liquid semiconductor which shows unusual electronic properties (a rapid change from semiconducting to metallic behaviour within 1 at.% of stoichiometry, and an anomalously low thermopower), also melts from a previously unreported superionic phase (Barnes *et al* 1994). In order to qualify and quantify theories based on this approach, more data are needed on the structure and ion dynamics from experimental measurements (e.g. quasi-elastic neutron scattering) and computer simulation techniques for a broader range of materials. The powerful AIMD method with its intrinsic calculation of the electronic structure and its ability to simulate off-stoichiometric compositions will prove to be particularly useful in understanding the complex nature of the electronic states in liquid semiconductors.

5. Conclusions

Despite its moderately high electronic conductivity the structure of molten Ag_2Se is consistent with that of an ionic 2:1 liquid consisting of predominantly Ag^+ and Se^{2-} ions. It is apparent, at the temperatures of this experiment, that the liquid is characterized by a well ordered Se–Se sub-structure with local coordinations typical of the fast-ion solid from which it melts. The Ag–Ag structure is consistent with a rapid movement of Ag^+ ions between the interstitial sites of this Se–Se sub-structure similar to that of the Ag^+ ions in the fast-ion solid. It is proposed that the high mobility of Ag^+ ions in Ag_2Se may produce an electronic carrier enhancement in the liquid which accounts for its unusual electronic properties.

It would be interesting to extend the study of this liquid to higher temperatures, in

particular to in excess of 1600 K. At this point the electronic properties become more 'conventional' and it is interesting to speculate whether the Se–Se sub-structure becomes sufficiently disordered to hinder the Ag^+ motion to such an extent that its diffusion coefficient becomes comparable to that of the Se^{2-} ion itself. This would be characterized by a significant decrease in the intensity of the first peak in $S_{SeSe}(Q)$ and by a relative sharpening of the peaks in $g_{AgAg}(r)$. At the same time a continuation of the computer simulation studies to these temperatures should be carried out.

Acknowledgments

This work was supported by the UK Engineering and Physical Sciences Research Council, which we gratefully acknowledge. One of us (SBL) gratefully acknowledges the University of Bristol for the award of a PhD scholarship. We would like to thank Professor Gillan and co-workers at the University of Keele for sending us the results of their *ab initio* molecular dynamics simulations and for many useful discussions about this technique. We would also like to thank Professor Enderby and Professor Evans at Bristol and Dr Silbert at Norwich for several useful discussions. Finally we would like to thank John Rowden for his help in preparing the sample containers.

References

Barnes A C 1993 *J. Non-Cryst. Solids* **156–158** 675
Barnes A C, Guo C and Howells W S 1994 *J. Phys.: Condens. Matter* **6** L467
Benmore C J and Salmon P S 1994 *Phys. Rev. Lett.* **73** 264
Bertagnolli H, Chieux P and Zeidler M D 1976 *Mol. Phys.* **32** 759
Bhatia A B 1977 *Liquid Metals 1976 (Inst. Phys. Conf. Ser. 30)* (Bristol: Institute of Physics Publishing) p 21
Bhatia A B and Thornton D E 1970 *Phys. Rev.* B **2** 3004
Biggin S and Enderby J E 1981 *J. Phys. C: Solid State Phys.* **14** 3129
Blech I A and Averbach B L 1965 *Phys. Rev.* A **137** 1113
Czack G, Koschel D and Kugier H H 1983 *Gmelin Handbook of Inorganic Chemistry, Silver Supplement* vol B3 (Berlin: Springer) pp 152–87
Edwards F G, Enderby J E, Howe R A and Page D I 1975 *J. Phys. C: Solid State Phys.* **8** 3483
Edwards F G, Howe R A, Enderby J E and Page D I 1978 *J. Phys. C: Solid State Phys.* **11** 1053
Enderby J E and Barnes A C 1990 *Rep. Prog. Phys.* **53** 85
Endo H, Yao M and Ishida K 1980 *J. Phys. Soc. Japan* **48** 235
Fortner J, Saboungi M-L and Enderby J E 1995 *Phys. Rev. Lett.* **74** 1415
Greaves G N, Gurman S J, Catlow C R A, Chadwick A V, Houde-Walter S, Henderson C M B and Dobson B R 1991 *Phil. Mag.* A **64** 1059
Hasegawa A 1985 *Solid State Ion.* **15** 81
Hawker I, Howe R A and Enderby J E 1974 *Amorphous and Liquid Semiconductors* ed J Stuke and W Brenig (London: Taylor and Francis)
Huberman B A 1974 *Phys. Rev. Lett.* **32** 1000
Jal J F, Mathieu C, Chieux P and Dupuy J 1990 *Phil. Mag.* B **62** 351
Kirchhoff F, Holender J M and Gillan M J 1996 *Phys. Rev.* B **54** 190
Kobayashi M 1990 *Solid State Ion.* **39** 121
Koester L and Knopf L 1980 *Z. Phys.* A **297** 85
Koester L, Knopf K and Waschkowski W 1980 *Z. Phys.* A **296** 43
McGreevy R L and Mitchell E W J 1982 *J. Phys. C: Solid State Phys.* **15** 5537
McGreevy R L and Pusztai L 1990 *Proc. R. Soc.* A **430** 241
Ohno S, Barnes A C and Enderby J E 1990 *J. Phys.: Condens. Matter* **2** 7707
——1994 *J. Phys.: Condens. Matter* **6** 5335
Paalman H H and Pings C J 1962 *J. Appl. Phys.* **33** 2635
Penfold I T and Salmon P S 1991 *Phys. Rev. Lett.* **67** 97
Poncet P J F 1977 *Institut Laue–Langevin (Grenoble) Report* 77PO15S

Poncet P J F 1978 *Institut Laue–Langevin (Grenoble) Report* 78P087S
Price D L, Saboungi M-L, Susman S, Volin K J, Enderby J E and Barnes A C 1993 *J. Phys.: Condens. Matter* **5** 3087
Ramasesha S 1982 *J. Solid State Chem.* **41** 333
Rino J P, Hornos Y M M, Antonio G A, Ebbsjö I, Kalia R K and Vashishta P 1988 *J. Chem. Phys.* **89** 7542
Rovere M and Tosi M P 1986 *Rep. Prog. Phys.* **49** 1001
Salmon P S 1992 *Proc. R. Soc.* A **437** 591
Salmon P S and Liu J 1996 *J. Non-Cryst. Solids* **205–207** 172
Soper A K and Egelstaff P A 1980 *Nucl. Instrum. Methods* **178** 415
Stillinger F H and Lovett R 1968 *J. Chem. Phys.* **49** 1991
Tsuchiya Y 1996 *J. Phys.: Condens. Matter* **8** 1897
Yarnell J L, Katz M J, Wenzel R G and Koenig S H 1973 *Phys. Rev.* A **7** 2130